ADAPTIVE CONTROL OF NONLINEAR VISUAL SERVOING SYSTEMS VIA IMAGE-BASED LINEARIZATION

Alessandro R. L. Zachi*, Liu Hsu†, Fernando Lizarralde†, Antonio C. Leite†

*Department of Electrical Engineering
Centro Federal de Educação Tecnológica Celso Suckow da Fonseca - CEFET/RJ
Rio de Janeiro, RJ, Brazil

†Department of Electrical Engineering/COPPE
Federal University of Rio de Janeiro
Rio de Janeiro, RJ, Brazil

Emails: zachi@coep.ufrj.br, liu@coep.ufrj.br, fernando@coep.ufrj.br, toni@coep.ufrj.br

Abstract— In this work, the adaptive control of nonlinear visual servoing systems is considered. The strategy is developed for eye-to-hand systems to perform positioning and tracking tasks on the 3D environment, when both camera calibration and robot parameters are uncertain. An image-based linearization method is introduced to deal with the nonlinear control problem generated by a time-varying depth. The positioning controller is then designed by using the recently proposed Immersion and Invariance (I&I) method, whereas the Symmetric-Diagonal-Upper (SDU) factorization method is adopted to solve the adaptive multivariable tracking control problem. The overall positioning/tracking controller is first developed for the cartesian robot case, and then extended to the general case. Simulation results are also presented for the proposed strategy.

Keywords— Nonlinear control, Adaptive Control, Uncertain systems, Visual servoing.

1 Introduction

For many years researchers have actively investigated the use of visual servoing in the control of robotic systems. The feedback provided by vision has been used to develop several stable control strategies (c.f.(Hutchinson et al., 1996)). For any choice of camera configuration, i.e., fixed (eye-to-hand) or moving camera (eye-in-hand), several other control schemes have been proposed to solve the problem of robot motion in the 3D environment (Espiau et al., 1992; Corke and Hutchinson, 2000; Kelly et al., 2000; Conticelli and Allotta, 2001). One restriction of some of the controllers cited above is that each of the results needs to use an available estimate of the depth information. For example, in (Malis et al., 1999) an off-line learning stage is required to estimate the distance of the desired camera position to the reference plane. In (Fang et al., 2002), this off-line phase is not required to determine the unknown depth distance since an estimate is obtained at each interaction by means of an *Euclidean homography* method.

Some works have considered the compensation for the lack of depth information, for instance, in (Conticelli and Allotta, 2001) an adaptive kinematic controller was designed to ensure uniformly ultimately bounded set-point regulation, provided that conditions on the translational velocities and bounds on the uncertain depth parameter are satisfied. In (Hsu et al., 2001), an adaptive stable controller was designed to allow tracking of trajectories over some smooth surfaces. Since the model becomes nonlinear due to the time-varying depth displacement, an appropriated function approximation was used in order to reach a suitable linear parameterized control structure.

In this work, a new 2D adaptive visual controller is considered. The proposed scheme is developed for image-based eye-to-hand systems to perform position and tracking tasks on the 3D environment, when both camera calibration and robot parameters are uncertain. The main interest of compensating for the lack of knowledge about the system parameters or environment, is to increase robot autonomy through sensor-based control without explicit human intervention or reprogramming. By extracting additional features from the image, an Image-Based Linearization algorithm is introduced to obtain a linearly parameterized plant description. The positioning task is then performed through the design of a stable adaptive Immersion and Invariance (I&I) controller. In order to solve the multivariable parameter adaptive tracking problem, the recently proposed Symmetric-Diagonal-Upper (SDU) factorization method (Costa et al., 2003) is used. The positioning/tracking controller is first developed for the cartesian robot case, in which all the image features are extracted from a planar landmark. The approach is then broaden to the general case by using a spherical landmark.

The paper is organized as follows: Section 2 describes the tasks to be achieved and presents the basic description of the visual servoing model. In Section 3, the Image-Based Linearization strategy is introduced and the adaptive I&I visual positioning controller is developed. Stability results for the positioning subsystem are also presented in this section. The SDU method is introduced in Section 4 to solve the adaptive visual tracking

control problem. The overall system stability is discussed. The simulation results obtained with the proposed strategy are shown in Section 5.

2 Problem Formulation

Consider the kinematic control problem of visually positioning a robotic system at a specific location while performing tracking of some desired trajectory using only a fixed (*eye-to-hand*) and uncalibrated camera, and with no available measurement of the depth distance $z(t)$.

2.1 Translational model

Provided that motions will be performed on a 3D environment, the image system has to control three degrees of freedom. Thus, at least, three independent features need to be extracted from the image in order to accomplish a specified position/tracking task, i.e., the centroid of an observed landmark and its projected surface. Since the landmark centroid is a physical point on the 3D space, its translational motion relatively to the camera frame can be described by the well-known relation (Hutchinson et al., 1996):

$$\begin{bmatrix} \dot{x}_{c1} \\ \dot{x}_{c2} \end{bmatrix} = \frac{1}{z} \begin{bmatrix} 1 & 0 & -x_{c1} \\ 0 & 1 & -x_{c2} \end{bmatrix} \begin{bmatrix} \dot{x} \\ \dot{y} \\ \dot{z} \end{bmatrix}, \quad (1)$$

where (x_{c1}, x_{c2}) is the centroid position in the camera frame, and $(\dot{x}, \dot{y}, \dot{z})$ is the vector of landmark translational velocities in the robot frame, where z is the total depth from the camera to the robot workspace. For the sake of simplicity, we consider the camera focal length $f = 1$. Also, we assume that the camera and robot frames have the same orientation with affine z-axis.

The dynamics of the landmark projected surface S_c in the camera frame has been considered in the work (Flandi et al., 2000) and, more recently in (Zachi et al., 2004), i.e.:

$$\dot{S}_c = -\left(\frac{2S_c}{z}\right)\dot{z}\,, \quad (2)$$

the overall dynamics of the positioning/tracking system will be given by:

$$\begin{bmatrix} \dot{x}_{c1} \\ \dot{x}_{c2} \\ \dot{S}_c \end{bmatrix} = \frac{1}{z} \underbrace{\begin{bmatrix} 1 & 0 & -x_{c1} \\ 0 & 1 & -x_{c2} \\ 0 & 0 & -2S_c \end{bmatrix}}_{L_0(s_T)} \begin{bmatrix} \dot{x} \\ \dot{y} \\ \dot{z} \end{bmatrix}, \quad (3)$$

where we denote the feature vector by $s_T = [x_c^T \; S_c]^T$, the translational velocity vector by $T = [\dot{x}, \dot{y}, \dot{z}]^T$, the meter-to-pixel transformation matrix by $A = diag\{f\alpha_1, f\alpha_2, f^2\alpha_1\alpha_2\}$ and an elementary rotation matrix $R_z(\phi) \in \Re^{3\times3}$ about z. But (3) can be described in a more complete form, namely:

$$\dot{s}_T = \frac{1}{z} L_T(s_T) T = \frac{1}{z} A L_0(s_T) R(\phi) T\,, \quad (4)$$

$$L_T(s_T) = \begin{bmatrix} \alpha_1 fc\phi & -\alpha_1 fs\phi & -\alpha_1 fx_{c1} \\ \alpha_2 fs\phi & \alpha_2 fc\phi & -\alpha_2 fx_{c2} \\ 0 & 0 & -2\alpha_1\alpha_2 f^2 S_c \end{bmatrix},$$

where $\alpha_1, \alpha_2 > 0$ are scaling factors, and $s\phi$, $c\phi$, are the simplified notations for $sin(\phi)$, $cos(\phi)$, respectively. The matrix $L_T(s_T)$ obtained in the above equation is also known as *translational Jacobian* (Hutchinson et al., 1996).

3 Adaptive Depth Positioning

In this section, the goal is to design an adaptive control law that drives the system to a specific depth position in accordance to a known desired image projected surface S_c^*. Note from (4) that $\dot{z}$ is the only control variable that interacts with S_c and then, a scalar control strategy can be adopted for the positioning problem. Here, we use the Adaptive Immersion and Invariance (I&I) method recently proposed in (Ortega et al., 2003). For the control design, we need to consider two basic assumptions:

Assumption 1 *The motions in the 3D environment are such that the observed landmark attached to the robot wrist is planar and always parallel to the image frame.*

Assumption 2 *The projected surface $S_c(t)$ of the landmark is assumed to be always within the image range $S_{max} > S_c(t) > S_{min} > 0$.*

3.1 Depth model

For the positioning model description, one can integrate both sides of (2) in the intervals $[S_{c_0}, S_c]$ and $[z_0, z]$, to obtain the following relationship:

$$z = z_0 \left(\frac{S_{c_0}}{S_c}\right)^{\frac{1}{2}}. \quad (5)$$

From (3), (4) and (5) we define a scaled version of the translational velocity vector T:

$$W = \begin{bmatrix} w_1 \\ w_2 \\ w_3 \end{bmatrix} = \left(\frac{S_c}{S_{c_0}}\right)^{\frac{1}{2}} T\,, \quad (6)$$

where S_{c_0} is a fixed image projected surface of the landmark, while S_c is continuously captured by the camera. Then, rewriting $\dot{S}_c$ based on (4), (5) and (6), we finally obtain the following (linear) system model:

$$\dot{S}_c = k_p \bar{w}_3\,, \quad (7)$$

with

$$k_p = -\alpha_1\alpha_2 f^2/z_0\,, \quad (8)$$

$$\bar{w}_3 = S_c w_3\,. \quad (9)$$

3.2 I&I control design

First, assuming that k_p has known sign, we rewrite the model (7) in a more suitable form:

$$\dot{S}_c = |k_p|\widehat{w}_3\,, \tag{10}$$

where we define

$$\widehat{w}_3 = sign(k_p)\bar{w}_3\,. \tag{11}$$

In order to apply the I&I design method, we need to use a first order filter of type

$$\Lambda_F(s) = \frac{\lambda_f}{s+\lambda_f}\,, \quad \lambda_f > 0\,, \tag{12}$$

to describe the system (10) in its filtered version

$$\dot{S}_{cf} = |k_p|\widehat{w}_{3f} + \varepsilon(t)\,, \tag{13}$$

where $\dot{S}_{cf}$ and $\widehat{w}_{3f}$ are the filtered versions of $\dot{S}_c$ and $\widehat{w}_3$, respectively, and $\varepsilon(t)$ is a vanishing term. Here, for the sake of simplicity, we assume that $\varepsilon(t) \equiv 0$. Thus, if the reference signals S_c^* and $\dot{S}_c^*$ are bounded and available, then the I&I control parameterization is given by (Ortega et al., 2003)

$$\widehat{w}_{3f*} = \underbrace{-|k_p|^{-1}}_{\theta_p^*}\underbrace{\left[\lambda_f e_{pf} - \dot{S}_{cf}^*\right]}_{\Psi_f(e_{pf})}\,, \tag{14}$$

with e_{pf}, $\dot{S}_{cf}^*$ and Ψ_f being the filtered (12) versions of the positioning error $e_p = S_c - S_c^*$, the reference surface velocity $\dot{S}_c^*$, and the regressor function $\Psi(e_p)$, respectively.

Since $|k_p|$ is uncertain, we define the (non certainty equivalent) control signal (Ortega et al., 2003)

$$\widehat{w}_{3f} = \Psi_f(e_{pf})[\theta_p + \beta_1(e_{pf})]\,, \tag{15}$$

where $\beta_1(e_{pf})$ is a function to be chosen.

If we define the parameter error to be

$$\nu := \theta_p - \theta_p^* + \beta_1(e_{pf})\,, \tag{16}$$

then (13) can be rearranged based on (14), (15) and (16), i.e.,

$$\begin{aligned}\dot{S}_{cf} &= |k_p|\widehat{w}_{3f} = |k_p|\Psi_f(e_{pf})[\nu + \theta_p^*] \\ &= |k_p|\Psi_f(e_{pf})\nu - \lambda_f e_{pf} + \dot{S}_{cf}^*\,,\end{aligned} \tag{17}$$

to reach

$$\dot{e}_{pf} = -\lambda_f e_{pf} + |k_p|\Psi_f(e_{pf})\nu\,. \tag{18}$$

Now, computing the derivative of (16), we have

$$\dot{\nu} = \dot{\theta}_p + \dot{\beta}_1(e_{pf})\,, \tag{19}$$

which by virtue of the convenient choices[1] of

$$\beta_1(e_{pf}) = -\Psi_f(e_{pf})\gamma_p e_{pf}\,, \tag{20}$$

and

$$\dot{\theta}_p = -[2\Psi_f(e_{pf}) - \Psi(e_p)]\gamma_p e_p\,, \tag{21}$$

reduces to

$$\dot{\nu} = -\gamma_p|k_p|\Psi_f^2(e_{pf})\nu\,, \quad \gamma_p > 0\,. \tag{22}$$

To test the stability of the error system composed by (18) and (22), we choose the following Lyapunov function with state $\xi = [e_{pf}, \nu]^T$:

$$V(\xi) = \frac{1}{2}e_{pf}^2 + \frac{\alpha}{2}\nu^2\,, \quad \alpha > 0\,. \tag{23}$$

The derivative of (23) along the trajectories of (18) and (22), is given by

$$\dot{V}(\xi) = -\lambda_f e_{pf}^2 + e_{pf}|k_p|\Psi_f\nu - \alpha\gamma_p|k_p|\Psi_f^2\nu^2\,. \tag{24}$$

If we define a new variable $\nu_\Psi = \Psi_f\nu$, then (24) reduces to

$$\dot{V}(\xi) = -\lambda_f e_{pf}^2 + e_{pf}|k_p|\nu_\Psi - \alpha\gamma_p|k_p|\nu_\Psi^2\,, \tag{25}$$

or, in a more compact form

$$\dot{V}(\eta) = -\eta^T B\eta\,, \tag{26}$$

where

$$B = \begin{bmatrix} \lambda_f & -\frac{1}{2}|k_p| \\ -\frac{1}{2}|k_p| & \alpha\gamma_p|k_p| \end{bmatrix}\,, \tag{27}$$

and $\eta = [e_{pf}, \nu_\Psi]^T$ is the new Lyapunov function state.

Then, applying the Schur´s Complement to B, we obtain the following conditions for the positive definiteness

$$\lambda_f > 0\,, \quad \alpha > \frac{|k_p|}{4\gamma_p\lambda_f}\,. \tag{28}$$

Although the negative definiteness of $-\eta^T B\eta$ with respect to η can be assured by choosing a sufficiently large term α, only negative semi-definiteness can be stated for (24) with respect to ξ. Indeed, from (24)-(26), we have that

$$\dot{V}(\xi) \leq -\xi^T\left(\Phi^T\mathcal{B}\Phi\right)\xi \leq 0\,, \tag{29}$$

with

$$\eta(\xi) = \Phi\xi\,, \quad \Phi = diag\{1, \Psi_f\}\,. \tag{30}$$

Then, based on the properties of the Lyapunov functions (23), (25) and also based on (30), we conclude that $\eta(t) \in \mathcal{L}_\infty$. If the second derivative of S_c^* is bounded, then by differentiating (26), one can verify from (14), (18), (22) and (30) that

$$\ddot{V}(\eta) = -2\eta^T B\dot{\eta}\,, \tag{31}$$

is bounded and use the *Barbalat's Lemma* to demonstrate that $\lim_{t\to\infty}\eta(t) \to 0$. From (18) and from the conclusions above, we can state that $\lim_{t\to\infty}\dot{e}_{pf}(t) \to 0$, which also implies from (12) that $\lim_{t\to\infty}e_p(t) \to 0$. In addition, from (16) and (30) we have that $\nu(t), \theta_p(t) \in \mathcal{L}_\infty$. Thus, we can finally conclude that all signals of the closed loop positioning subsystem are uniformly bounded.

[1] For a detailed description see reference (Ortega et al., 2003)

3.3 Control law

To restore $\widehat{w}_3(t)$ from (15), one can use (12) and the following property

$$\frac{d}{dt}\left[\theta_p - \gamma_p \Psi_f e_{pf}\right] = -\gamma_p \Psi_f e_p, \tag{32}$$

to obtain

$$\widehat{w}_3(t) = \Psi\theta_p - \gamma_p \Psi\Psi_f e_{pf} - \Psi_f^2 e_p\,. \tag{33}$$

Thus, the true cartesian control signal $\dot{z}(t)$ (4), can be simply computed from (33) by successive substitutions into (11), (9) and (6), respectively.

4 Adaptive Planar Tracking

Once we have shown that the system can be properly positioned by the adaptive I&I controller developed in the previous section, our goal now is to perform asymptotic tracking of some predefined image trajectory. However, as can be observed from (4), both x_{c1} and x_{c2} interacts with all the components of the scaled control W, thus generating a coupled multivariable subsystem. Indeed, reproducing the first two rows of the nonlinear system (4), also based on (5) and (6), we have:

$$\dot{x}_c = K_T u + G_T w_T\,, \tag{34}$$

with

$$K_T = \frac{f}{z_0}\begin{bmatrix} \alpha_1 c\phi & -\alpha_1 s\phi \\ \alpha_2 s\phi & \alpha_2 c\phi \end{bmatrix}, \quad u = \begin{bmatrix} w_1 \\ w_2 \end{bmatrix},$$

$$G_T = \frac{f}{z_0}\begin{bmatrix} -\alpha_1 & 0 \\ 0 & -\alpha_2 \end{bmatrix}, \quad w_T = w_3 \begin{bmatrix} x_{c1} \\ x_{c2} \end{bmatrix},$$

which consists of a *linearly parameterized* tracking system. Then, an adequate control parameterization must follows since now we are dealing with matricial control gains instead of scalar ones. Some works have gone toward this issue (Ioannou and Sun, 1996), however assuming restrictive conditions and/or conditions very difficult to satisfy in practice (a detailed discussion about such conditions can be found in (Hsu and Costa, 1999)). Most recent methods have proven to be less restrictive (Hsu and Costa, 1999; Costa et al., 2003; Ortega et al., 2003). Here, we will adopt the one introduced in (Costa et al., 2003), which uses a *Symmetric-Diagonal-Upper (SDU) factorization* of the system gain matrix.

4.1 Control design

In this section, the control design will follow the one in (Zachi et al., 2004). For the subsystem (34), consider the following reference model

$$\begin{aligned} \dot{x}_{c_M} &= -\lambda_M x_{c_M} + \lambda_M r_c(t)\,, && (35)\\ y_{c_M} &= x_{c_M}\,, && (36) \end{aligned}$$

where $\lambda_M > 0$ and $r_c(t) \in \Re^2$ is a bounded exogenous reference signal. The ideal control signal u^* that perfectly matches (34) and (35), is given by:

$$u = u^* = K_T^{-1}\left[\lambda_M(r_c - x_c) - G_T w_T\right] = P^*\sigma\,, \tag{37}$$

with

$$\begin{aligned} P^* &= \begin{bmatrix} p_{11}^* & p_{12}^* & p_{13}^* & p_{14}^* \\ p_{21}^* & p_{22}^* & p_{23}^* & p_{24}^* \end{bmatrix}, && (38)\\ \sigma &= \begin{bmatrix} (r_c - x_c)^T & w_T^T \end{bmatrix}^T. && (39) \end{aligned}$$

Since P^* is an uncertain matrix, we use the *certainty equivalence principle* to design u as

$$u = P\sigma\,, \tag{40}$$

where P is the matrix of the adaptive parameters p_{ij}. Thus, the error equation is obtained by adding and subtracting (37) into (34), i.e.,

$$\begin{aligned} \dot{x}_c &= K_T u + G_T w_T + K_T u^* - K_T u^* = \\ &= -\lambda_M x_c + \lambda_M r_c + K_T(u - u^*)\,. && (41) \end{aligned}$$

Denoting $\tilde{u} = u - u^*$, $e_c = x_c - x_{c_M}$ and subtracting (35) from (41), we finally reach:

$$\dot{e}_c = -\lambda_M e_c + K_T\tilde{u}\,. \tag{42}$$

4.2 Parameterization via SDU factorization

According to (Costa et al., 2003), if K_T has nonzero principal minors, then it is always possible to factorize K_T as:

$$K_T = SDU\,, \tag{43}$$

where S denotes a *symmetric* and positive definite matrix, D denotes a *diagonal* matrix and U an *unitary upper triangular* one. Then, from (41) and (43) we can write

$$\begin{aligned} \dot{e}_c &= -\lambda_M e_c + SDU(u - P^*\sigma) \\ &= -\lambda_M e_c + SD(Uu - UP^*\sigma)\,. && (44) \end{aligned}$$

Here, employing the decomposition $Uu = u - (I - U)u$ we also have:

$$\dot{e}_c = -\lambda_M e_c + SD[u - \Lambda\sigma - (I - U)u]\,, \tag{45}$$

with $\Lambda = UP^*$. If we introduce a new ideal control vector

$$\begin{bmatrix} \Theta_1^{*T}\Omega_1 \\ \Theta_2^{*T}\Omega_2 \end{bmatrix} \equiv \Lambda\sigma + (I - U)u\,, \tag{46}$$

where $\Omega_1 = [\sigma^T, u_2]^T$ and $\Omega_2 = \sigma$, the error equation (45) reduces to

$$\dot{e}_c = -\lambda_M e_c + SD\left(u - \begin{bmatrix} \Theta_1^{*T}\Omega_1 \\ \Theta_2^{*T}\Omega_2 \end{bmatrix}\right), \tag{47}$$

from which we can extract the final control parametrization:

$$u = [\Theta_1^T\Omega_1\,, \Theta_2^T\Omega_2]^T\,. \tag{48}$$

4.3 Adaptation laws

Based on the factorization properties discussed in (Costa et al., 2003), we assume that the entries of $D = diag\{d_1, d_2\}$ have known signs. Since S is a symmetric and positive definite matrix, we follow the standard Lyapunov design by choosing the following Lyapunov function candidate

$$2V(e_c, \tilde{\Theta}) = e_c^T S^{-1} e_c + \gamma^{-1} \sum_{i=1}^{2} (|d_i| \tilde{\Theta}_i^T \tilde{\Theta}_i) \,. \quad (49)$$

The time derivative of (49) along (47) yields:

$$\dot{V}(e_c, \tilde{\Theta}) = -\lambda_M e_c^T S^{-1} e_c + \sum_{j=1}^{2} (e_{cj} d_j \tilde{\Theta}_j^T \Omega_j) + \gamma^{-1} \sum_{i=1}^{2} (|d_i| \tilde{\Theta}_i^T \dot{\tilde{\Theta}}_i). \quad (50)$$

Then, by choosing the adaptation laws as:

$$\dot{\tilde{\Theta}}_i = -\gamma sign(d_i) e_{c_i} \Omega_i \,, (i = 1, 2) \,, \quad (51)$$

equation (50) reduces to

$$\dot{V}(e_c, \tilde{\Theta}) = -\lambda_M e_c^T S^{-1} e_c \leq 0 \,. \quad (52)$$

From (49) and (52), we conclude that $e_c(t), \tilde{\Theta}(t) \in \mathcal{L}_\infty$, which imply that $x_c(t), \Theta(t) \in \mathcal{L}_\infty$. From the boundedness properties of (39), (47) and (48), we verify that the second derivative of $V(e_c, \tilde{\Theta})$ is also bounded. Then, by *Barbalat's Lemma*, one can note that $\lim_{t\to\infty} e_c(t) \to 0$. Thus, the convergence and boundedness properties of all the closed loop signals can be demonstrated. At this point, the results obtained for the positioning subsystem (Sections 3) and those obtained for the tracking subsystem can be put together and lead to the following overall result:

Theorem 1 *Consider the adaptive visual servoing system composed by (4), the reference model described by some S_c^* and (35), the control laws (33), (48), and the adaptation laws (21), (51). If the camera misalignment angle $\phi \in (-\pi/2, \pi/2)$ then: (a) all the closed loop signals are uniformly bounded; (b) for $\zeta(t) := [e_c^T, e_p]^T$, $\zeta(t) \in \mathcal{L}_2 \bigcap \mathcal{L}_\infty$, $\lim_{t\to\infty} \zeta(t) \to 0$.*

Remark 1 *(General Robotic Systems) In the previous sections, the key reason to adopt Assumption 1 was to exclude rotational motions of the landmark, assuring that its projected surface only changes with depth. Indeed, it is well-known from (Haralick and Shapiro, 1993, page 50) that rotations of planar objects relatively to the image plane generate changes in the image projected surface. It is important to stress that, in general robotic systems in which object rotations are performed, relation (5) is not valid. However, if a spherical landmark is used instead of the planar one, it is possible to broaden the proposed strategy to consider the general case. In fact, adopting this special landmark, image projected surfaces become invariant over any kind of object rotation, thus forcing them to change only with depth. Note that in this case relation (5) is still valid and can be used.*

5 Simulation Results

In order to illustrate the performance of the proposed adaptive scheme, we consider a visual servo system with the following parameters: $f = 0.006$, $\phi = \pi/6$, $\alpha_1 = \alpha_2 = 83$. Also we consider $S_{c0} = 1$ for $z_0 = 1$. For the adaptive controllers (21),(33) and (48),(51), we assign $\gamma = 20$ and $\gamma_p = 0.4$. Other simulation parameters are set to: $\lambda_f = 0.1$; $\lambda_M = 2$; $S_c^* = 1$; $r_{c1}(t) = sin(0.5t)$; $r_{c2}(t) = cos(0.5t)$; $\theta_p(0) = 0$; $\Theta_1(0) = [0, 0, 0, 0, 0]^T$; $\Theta_2(0) = [0, 0, 0, 0]^T$.

The Figures 1-3 illustrate the behavior of such controller. The asymptotic convergence of the positioning and tracking errors are graphically clear from Fig. 1. As can be deduced from figure 1, the adaptive parameters (not illustrated) tend to a steady state value after a learning period. Control signals for positioning and tracking are shown in Fig. 2. It is important to discuss that in the present I&I regulation controller, we can tune λ_f and γ_p in order to improve steady-state performance. A rigorous explanation for this peculiarity can be found in the original work (Ortega et al., 2003).

The robot frame trajectories during the positioning/tracking task are shown in Fig. 3.

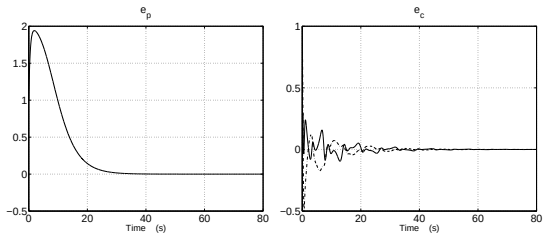

Figure 1: Positioning/tracking errors.

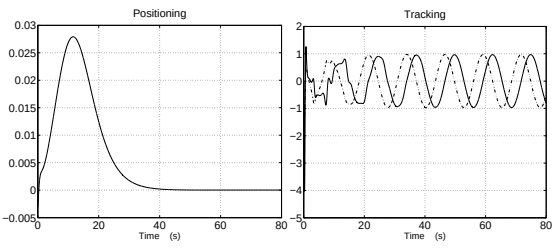

Figure 2: Cartesian control signals for positioning/tracking.

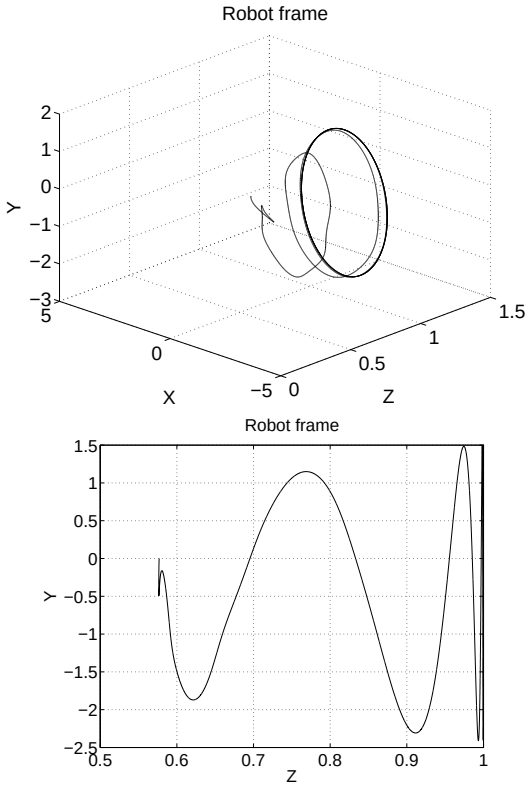

Figure 3: End-effector trajectory.

6 Conclusion

In this paper, we have developed a novel 2D adaptive visual servoing scheme that provides stable position/tracking tasks for robot manipulator systems. The controller was first designed for the cartesian robot case, in which all the image features are extracted from a planar landmark. For the scalar positioning subsystem, the novel I&I control method was applied. For the multivariable tracking subsystem, the recently proposed *SDU factorization* method was adopted. By using a spherical landmark instead of a planar one, the position/tracking approach was broaden to include the general case of robotic systems. The stability analysis for the proposed strategy was also presented. Simulation results were included to illustrate the performance of the proposed strategy.

References

Bishop, B., Spong, M. (1997). "Adaptive calibration and control of 2D monocular visual servo systems," in *Proc. of Syroco97*.

Conticelli, A., Allotta, B. (2001). "Discrete-Time Robot Visual Servoing in 3-D Positioning Tasks With Depth Adaptation", in *IEEE/ASME Trans. on Mechatronics*, vol. 6, no. 3, pp. 356-363.

Conticelli, A., Allotta, B. (2001). "Nonlinear Controllability and Stability Analysis of Adaptive Image-Based Systems", in *IEEE Trans. on Robotics and Automation*, vol. 17, no. 2, pp. 208-214.

Corke, P. I., Hutchinson, S. A. (2000). "A New Hybrid Image-Based Visual Servo Control Scheme", in *Proc. IEEE Conf. on Dec. and Control*, pp. 2521-2527.

Costa, R. R., Hsu, L., Imai, A., Kokotovic, P. (2003). "Lyapunov-based adaptive control of MIMO systems", in *Automatica*, vol. 39, Issue 7, pp. 1251-1257.

Espiau, B., Chaumette, F., Rives, P. (1992). "A new approach to visual servoing in robotics", in *IEEE Trans. on Robotics and Automation*, vol. 8, June, pp. 313-326,

Fang, Y., Behal, A., Dixon, W. E., Dawson, D. M. (2002). "Adaptive 2.5D Visual Servoing of Kinamatic Redundant Robot Manipulators", in *Proc. IEEE Conf. on Dec. and Control*, (Las Vegas, Nevada), pp. 2860-2865.

Flandin, G., Chaumette, F., Marchand, E. (2000). "Eye-in-hand/Eye-to-hand Cooperation for Visual Servoing", in *Proc. IEEE Conf. on Robotics and Automation*, (San Francisco, CA), pp. 2741-2746.

Haralick, R. M., Shapiro, L. G. (1993). "Computer and Robot Vision", Addison-Wesley.

Hsu, L. and Aquino, P.(1999)."Adaptive visual tracking with uncertain manipulator dynamic and uncalibrated camera," in *Proc. IEEE Conf. on Dec. and Contr.*, pp. 1248–1253.

Hsu, L. and Costa, R.(1999)."MIMO direct adaptive control with reduced prior knowledge of the high frequency gain," in *Proc. IEEE Conf. on Dec. and Contr.*, pp. 3303–3308.

Hsu, L., Zachi, A. R. L. and Lizarralde, F.(2001). "Adaptive visual tracking for motions on smooth surfaces," in *Proc. IEEE Conf. on Decision and Control*, (Orlando, Flórida).

Hutchinson, S., Hager, G. and Corke, P.(1996)."A tutorial on visual servo control", in *IEEE Trans. Robotics and Automation*, vol. 12, no. 5, pp. 651–670.

Ioannou, P. and Sun, K.(1996). Robust Adaptive Control.Prentice Hall.

Kelly, R., Reyes, F., Moreno, J. *et al.*(1999)."Two Loops Direct Visual Control of Direct-Drive Planar Robots with Moving Target", in *Proc. of IEEE Int. Conf. on Robotics and Automation*.

Kelly, R., Carelli, R., Nasisi, O., Kuchen, B., Reyes, F.(2000)."Stable Visual Servoing of Camera-in-Hand Robotic Systems", in *IEEE/ASME Trans. on Mechatronics*, vol. 15, no. 1, pp. 39-48.

Koivo, A. and Houshangi, N.(1991)."Real-time vision feedback for servoing of a robotic manipulator with self-tuning controller", in *IEEE Trans. Syst., Man, Cybern.*, vol. 21, pp. 134–142.

Malis, E., Chaumette, F., Boudet, S.(1999)."2 1/2D Visual Servoing", in *IEEE Trans. on Robotics and Automation*, vol. 15, no. 2, pp. 238–250.

Ortega, R. Hsu, L., Astolfi, A.(2003)."Immersion and Invariance Adaptive Control of Linear Multivariable Systems", in *Systems and Control Letters*, vol. 49, pp. 37–47.

Sanderson, A. C., Weiss, L. E., Neuman, C. P.(1987)."Dynamic sensor-Based Control of Robots With Visual Feedback", in *IEEE Trans. on Robotics and Automation*, vol. RA3, October, pp. 404–417.

Sastry, S. S. and Bodson, M.(1989). Adaptive Control: Stability, Convergence and Robustness.Prentice Hall.

Soato, S., Frezza, R., Perona, P.(1996)."Motion Estimation Via Dynamical Vision", in *IEEE Trans. on Autom. Control*, vol. 41, no. 3, pp. 393–413.

Spong, M. W. and Vidyasagar, M.(1989). Robot Dynamics and Control.Wiley&Sons.

Zachi, A. R. L., Hsu, L., Lizarralde, F.(2004)."Performing Stable 2D Adaptive Visual Positioning/Tracking Control Without Explicit Depth Measurement", in *Proc. of IEEE Int. Conf. on Robotics and Automation*,pp.2297-2302, New Orleans (LA).